

Estimation of the Cartilage Volume Loss Due to Knee Osteoarthritis - Case Study

Suzana Petrovic Savic^a, Nikola Prodanovic^{b,c}, Vladimir Kocovic^a, Tijana Prodanovic^{d,e}, Dragan Dzunic^{a,*}, Branko Ristic^{b,c}, Goran Devedzic^a

^aFaculty of Engineering University of Kragujevac, Department for production engineering, Sestre Janjic 6, Kragujevac, Serbia,

^bFaculty of Medical Sciences University of Kragujevac, Department of Surgery, Svetozara Markovica 69, Kragujevac, Serbia,

^cUniversity Clinical Center Kragujevac, Clinic for Orthopaedic and Trauma Surgery, Zmaj Jovina 30, Kragujevac, Serbia,

^dFaculty of Medical Sciences University of Kragujevac, Department of Pediatrics, Svetozara Markovica 69, Kragujevac, Serbia,

^eUniversity Clinical Center Kragujevac, Pediatric Clinic, Center for Neonatology, Zmaj Jovina 30, Kragujevac, Serbia.

Keywords:

Osteoarthritis
Reverse engineering
Cartilage
Wear volume
Wear area

ABSTRACT

Osteoarthritis (OA) is a degenerative disease of the knee joint caused by the formation of cracks within the collagen fibers of the articular cartilage. Current research is directed towards less invasive procedures for treating this degenerative disease using tissue engineering and 3D bioprinting. Therefore, it is crucial to obtain the exact shape of the damaged tissue, reconstruct the original shape of the tissue, and estimate the volume and area resulting from the wear of the contact surfaces. The study used the tibial plateau of a patient with OA that was removed during total knee arthroplasty, and the data was collected using a 3D scanner. After the reconstruction of the tibial plateau, an assessment of the area and volume of wear on the medial condyle of the tibia was performed, along with a FEM analysis of the real and approximate shape of the cartilage tissue. In this way, it is possible to simulate and create a patient-specific 3D model with a reconstructed wear volume, which can be highly attractive for future treatment strategies for cartilage damage or early stages of OA.

* Corresponding author:

Dragan Dzunic 
E-mail: dzuna@kg.ac.rs

Received: 12 January 2023

Revised: 17 February 2023

Accepted: 7 March 2023

© 2023 Published by Faculty of Engineering

1. INTRODUCTION

The complex structure of healthy cartilage in the knee joint provides tolerance to the pressures, such as those caused by weight, to which the knee joint is exposed. In addition, the synovial fluid inside the knee joint

facilitates movement and reduces friction between the contact surfaces of the tibial cartilage and the femoral cartilage. However, if there is damage to the knee joint, which can accumulate over time, it creates conditions for the occurrence of osteoarthritis (OA). The development of OA is also influenced by joint

malformations, obesity, and disorders of the LE (lower extremity) axis [1-3].

Osteoarthritis (OA) is a chronic degenerative disease of the knee joint characterized by progressive loss of articular cartilage in depth due to the formation of cracks in the collagen fibers. Furthermore, OA of the knee joint is often accompanied by a disorder of the axis of the lower extremity. Specifically, dominant damage to the articular cartilage of the medial compartment of the knee is most often a consequence of varus knee deformity [4-6].

The progression of osteoarthritis (OA) leads to direct contact between the femur and the tibia, which further conditions bone remodeling, the formation of osteophytes, and reduced lubrication capabilities. This environment leads to different tribological performances within the joint, which are reflected in the increase of contact stresses and pressure in the knee joint due to degradation. The clinical manifestation of OA is reflected in the appearance of pain, stiffness, and reduced movement in the knee joint, which consequently affects the quality of life [1,6].

The diagnosis of knee osteoarthritis (OA) is most often based on radiography of the knee, although gait analysis of such patients using optical systems is also described in the literature [7,8].

Generally, cartilage has a reduced capacity for repair and is a challenge in treatment. Previous research has explored the use of various materials such as polymer hydrogels, polymer scaffolds, double-layer hydrogels, and cell therapy to repair articular cartilage for minor local lesions on the condyles or to restore synovial fluid [1,9]. However, with the appearance of abnormalities in the knee joint that cause large defects in the cartilage, there is an increase in the wear process [10].

Different types of wear can occur in the knee joint and are generally categorized as adhesive, abrasive, and fatigue wear. Adhesive wear is directly related to the contact of the loaded surfaces of the tibia and femur. Although synovial fluid is present as a lubricant between them, it can "split" due to the high specific value of contact pressure at

the point of contact. Abrasive wear implies the removal of particles from the surfaces of the articular cartilage that are in contact. Fatigue wear occurs due to the mechanism of movement within the knee joint, i.e. rolling and sliding. Cycles of variable loads to which the knee joint is exposed almost every day, as well as compressive and stretching stresses, can cause surface and subsurface cracks [1,11].

Tissue engineering and 3D bioprinting technologies offer a promising solution for the creation of patient-specific tissues with native tissue architecture. To achieve this, an adequate selection of cells and biomaterials is crucial, as well as the use of ideal scaffolds that meet specific conditions such as biocompatibility, biodegradability, and porosity. Current research in the field of tissue engineering focuses on the creation of mature tissue by growing cells inside optimal scaffolds. Particularly important is the exact shape of the damaged area, which must be precisely replicated for successful implantation [9,12].

As mentioned, ensuring precise shape and volume of the damaged area is essential in tissue engineering and 3D bioprinting, and reverse engineering technologies play a significant role in achieving this goal. These technologies can provide diagnostically valuable information related to tissue structure function. Virtual models of different tissue types can be reconstructed using MRI or CT records or scanned point clouds, depending on whether the tests were performed in vitro or in vivo. The resulting models can be used for various simulation analyses, such as reconstructing the previous state of the tissue or predicting future behavior [1,2,12-14].

The focus of this paper is on the utilization of reverse engineering to evaluate the extent of area and volume loss of cartilage tissue in the knee joint caused by osteoarthritis. Additionally, a comparative finite element analysis (FEA) was conducted to provide a comprehensive understanding of the condition of patients with this degenerative disease. The aim is to offer critical observations that could assist in future diagnoses and treatment options for patients.

2. MATERIALS AND METHODS

2.1 Participants

The study analyzed the progression of knee osteoarthritis in a patient after initial diagnosis. The patient's first examination showed early osteoarthritic changes on radiographs. After three years of follow-up, the patient's complaints progressed, leading to a varus deformity of the knee and consequent OA. The patient was evaluated clinically, radiographically, and

surgically by a specialist at the University Clinical Center in Kragujevac, following the Helsinki Declaration and good clinical practice with local Ethical Committee approval.

The Kellgren-Lawrence method was used to classify the patient's OA by analyzing radiographs. This method involves five categories (0, 1, 2, 3, 4), and a category 3 or 4 classification, along with pronounced symptoms of the disease, indicates a need for total knee arthroplasty (as shown in Fig. 1) [15,16].

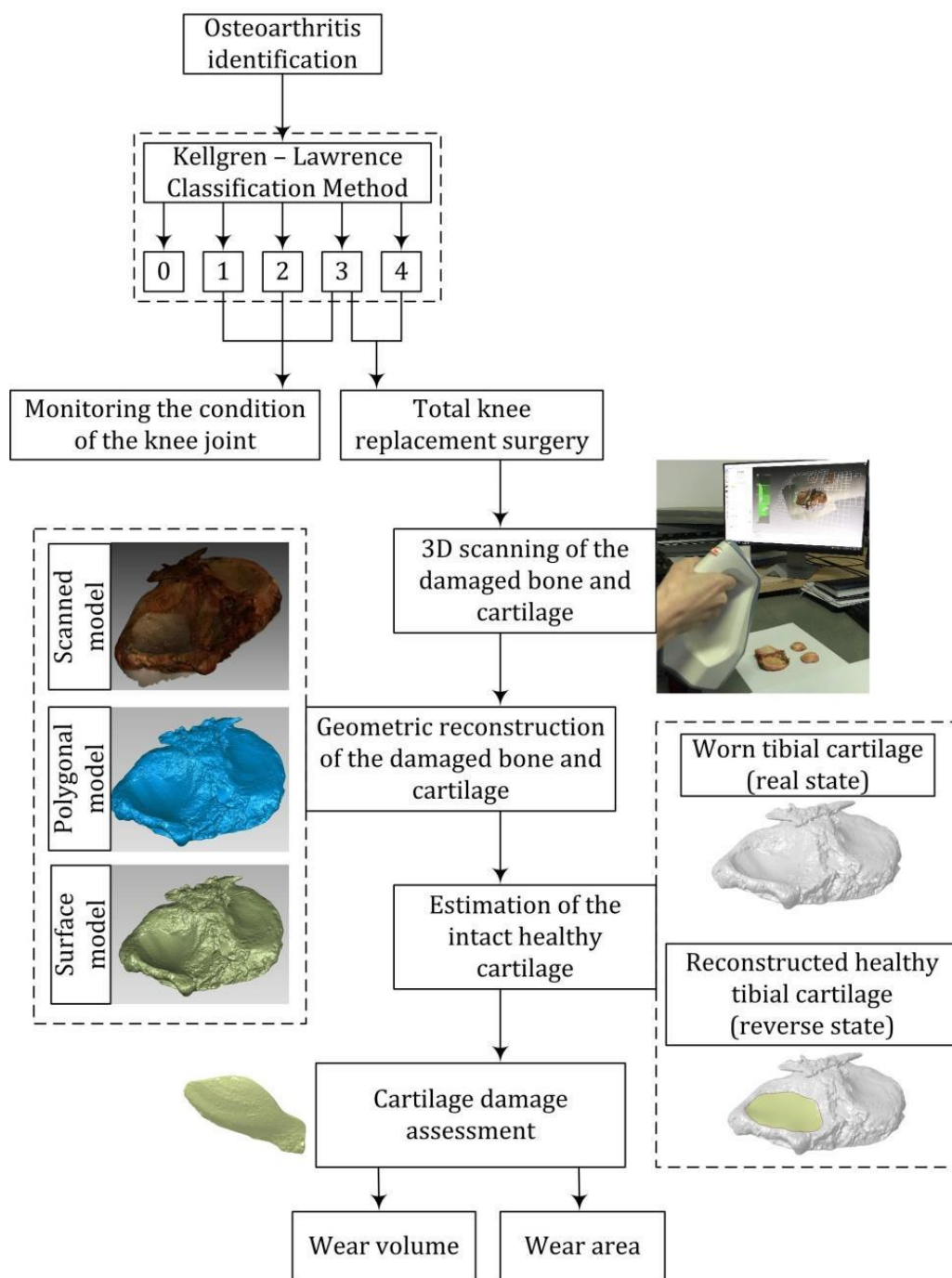


Fig. 1. Algorithm for assessment of tibial damage.

2.2 Scanning and processing of data

The Center for Integrated Product and Process Development and Intelligent Systems at the Faculty of Engineering, University of Kragujevac was responsible for data scanning and processing. The Artec Spider 3D scanner (www.artec3d.com) was used to scan the affected area of the tibia and epicondyle of the femur. This scanner can acquire data at a speed of 1,000,000 points/sec, with a 3D resolution of up to 0.1mm, and a precision of 3D points up to 0.03mm.

Processing, optimization, and geometric reconstruction of the scanned objects were performed using the Geomagic Design X software. After obtaining the optimal geometric shape of the scanned objects, the created surfaces were exported for further processing in the Catia V5 R21 software. The aim was to create a volume model of the tibia, reconstruct the original shape of the cartilage, and evaluate the volume of the worn cartilage

The algorithm for assessing damage to the tibia is shown in Fig. 1.

The determination of the volume and area of damage to the tibial condyle is based on visual identification of the lesion on both real and virtual models (Fig. 2). After aligning the wear zone, the boundary line between the damaged and undamaged parts of the cartilage is detected using a spline. These curves cover a wide range of functions used in applications where data interpolation and/or smoothing is required [17,18].

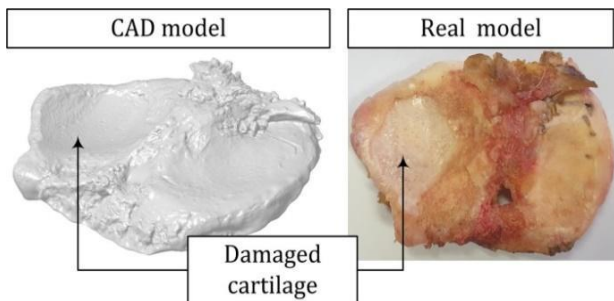
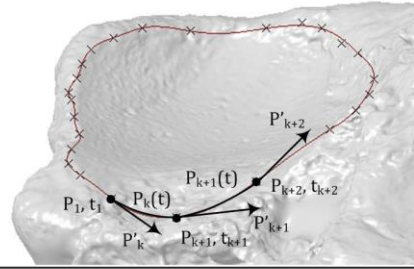


Fig. 2. Lesion identification on real and virtual models.

A cubic spline was used to create the boundary line, and an arbitrary segment was drawn and shown in Fig. 3.



Legend:
 P_1, P_{k+1}, P_{k+2} - Vector position of the points,
 P'_k, P'_{k+1}, P'_{k+2} - Tangents at points,
 t_k, t_{k+1}, t_{k+2} - Parameters,
 $P_k(t), P_{k+1}(t)$ - Segments.

Fig. 3. Spline segments.

Points on a spline segment are defined by the expression:

$$P_k(t) = \sum_{i=1}^4 B_{ik} t^{i-1}, \quad 0 \leq t \leq t_{k+1}, \quad 1 \leq k \leq n-1 \quad (1)$$

$$P_k(t) = \begin{bmatrix} 1 & t & t^2 & t^3 \end{bmatrix} \begin{bmatrix} B_{1k} \\ B_{2k} \\ B_{3k} \\ B_{4k} \end{bmatrix}, \quad (2)$$

where $B_{1k}, B_{2k}, B_{3k},$ and B_{4k} are coefficients that are calculated according to the following expression:

$$[B] = \begin{bmatrix} B_{1k} \\ B_{2k} \\ B_{3k} \\ B_{4k} \end{bmatrix} = \begin{bmatrix} 1 & 0 & 0 & 0 \\ 0 & 1 & 0 & 0 \\ -\frac{3}{t_{k+1}^2} & -\frac{2}{t_{k+1}} & \frac{3}{t_{k+1}^2} & -\frac{1}{t_{k+1}} \\ \frac{2}{t_{k+1}^3} & \frac{1}{t_{k+1}^2} & -\frac{2}{t_{k+1}^3} & \frac{1}{t_{k+1}^2} \end{bmatrix}. \quad (3)$$

By substituting the values for the coefficients in equation (2), it is obtained:

$$P_k(\tau) = \begin{bmatrix} F_1(\tau) & F_2(\tau) & F_3(\tau) & F_4(\tau) \end{bmatrix} \begin{bmatrix} P_k \\ P_{k+1} \\ P'_k \\ P'_{k+1} \end{bmatrix}, \quad (4)$$

$$0 \leq \tau \leq 1 \quad i \quad 0 \leq k \leq n-1$$

Where:

τ = Parameter dependent on parameter t and can be expressed using the relation:

$$\tau = \frac{t}{t_{k+1}}, \quad (5)$$

$F_{1k}, F_{2k}, F_{3k}, F_{4k}$ = Blending functions which are calculated according to the expressions:

$$F_{1k}(\tau) = 2\tau^3 - 3\tau^2 + 1, \quad (6)$$

$$F_{2k}(\tau) = -2\tau^3 + 3\tau^2, \quad (7)$$

$$F_{3k}(\tau) = \tau(\tau^2 - 2\tau + 1)t_{k+1}, \quad (8)$$

$$F_{4k}(\tau) = \tau(\tau^2 - \tau)t_{k+1}. \quad (9)$$

The damaged segment of cartilage (lesion) is located inside a defined spline, while outside of it, there is a healthy segment of cartilage. To fill the interior of the contour with a surface, the spatial position and curvature of the contour (i.e. intact cartilage) are followed, and the intact cartilage is approximated using a NURBS surface (Fig. 4). The NURBS surface is described by a relation that helps achieve the filling of the contour's interior with a surface [19]:

$$C(u) = \frac{\sum_{i=1}^n \sum_{j=0}^{n'} w_{ij} N_{i,k}(u) N'_{j,k}(v) \overline{P_{i,j}}}{\sum_{i=1}^n \sum_{j=0}^{n'} w_{ij} N_{i,k}(u) N'_{j,k}(v)}, \quad (10)$$

Where:

w_{ij} = Weight coefficients,

$P_{i,j}$ = Control points,

$N_{i,k}(u), N_{j,k}(v)$ = B - spline basis functions.

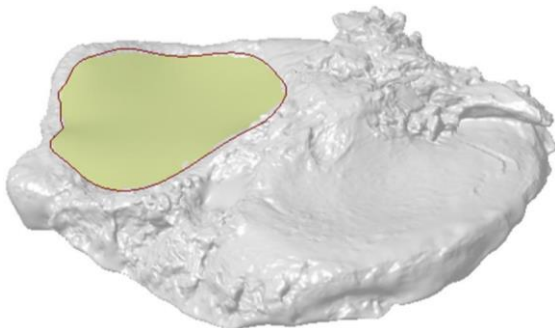


Fig. 4. Reconstructed tibial cartilage.

The process of defining the wear area and volume of the cartilage involves several steps (Fig. 5):

1. The first step is to detach the lesion on the tibia, which is bordered by a curve.
2. Next, the approximate surface of the intact cartilage and the lesion-extracted surface are joined together to create a single surface.

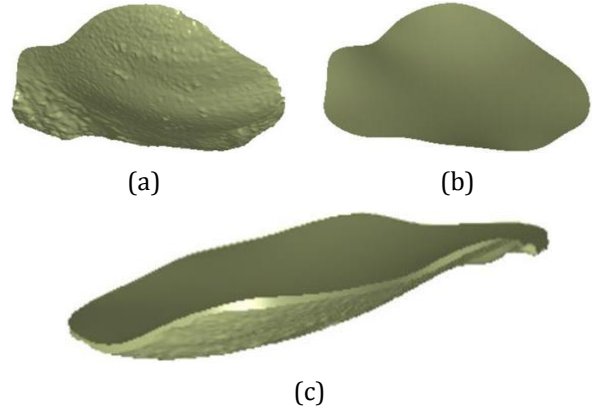


Fig. 5. Segments of the tibial spatial wear surface: (a) Extracted surface, (b) Reconstructed surface, and (c) Joined surface.

The surface of the damage is materialized by creating a volume model and defining the basic cartilage parameters such as Young's modulus ($E=12\text{MPa}$), Poisson's coefficient ($\nu=0.45$), and density ($1.26765\text{e-}9 \text{ ton/mm}^3$) [20]. These parameters allow for the determination of the area, mass, and volume of the wear.

With the defined cartilage parameters, a finite element analysis corresponding to the standing phase of the patient during support on one leg is performed.

3. RESULTS

The spatial representation of the tibial cartilage wear volume is illustrated in both Fig. 5 and Fig. 6. The dimples, which were formed due to improper loading resulting in deformation, are represented by a smooth surface approximation. The characteristic parameter values can be found in Table 1.

Table 1. Characteristic parameters.

Parameter	Value
Total area of the reconstructed cartilage volume, mm ²	2023.6
Area of the worn cartilage, mm ²	1208,9
Volume of the worn cartilage, ml	1.74
Mass of the worn cartilage, kg	0.012

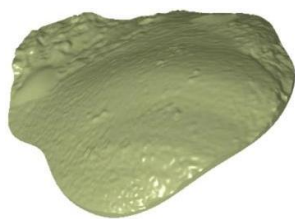


Fig. 6. Extracted cartilage volume.

To compare the stress distribution on the damaged cartilage and the reconstructed cartilage, we conducted FEM analysis while simulating the standing phase. This means that we only considered the effect of weight on the cartilage. In the damaged tibial condyle (Fig. 7), the stresses are unevenly distributed due to the deformity caused by OA. Notably, the maximum stresses of 25.1MPa are oriented in the anterior and medial directions, with the central part bearing little to no load.

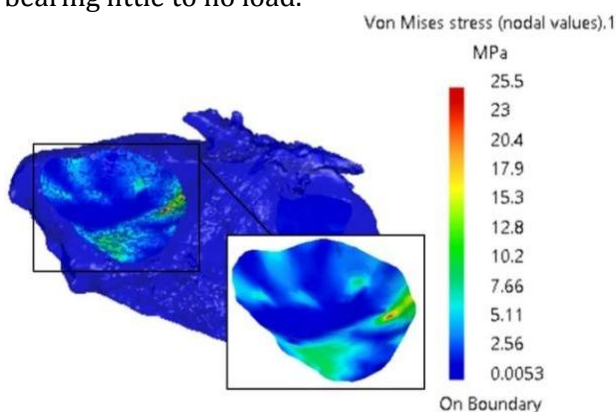


Fig. 7. Von Misses stress on worn tibial cartilage.

After reconstructing the geometry of the damaged cartilage, FEM analysis tests were conducted under the same conditions as for the damaged cartilage. The results show a significant reduction in the Von Misses stress values (Fig. 8). The maximum stress is now 7.16MPa, located in the central part of the tibial cartilage and transferred to the outer surfaces, where the stress decreases.

The different locations and stress values obtained by assessing the intact geometric shape of the cartilage suggest the potential for improving daily activities and reducing pain.

4. DISCUSSION

Numerous studies have focused on the prevalence of OA and its detrimental impact on daily life activities. As people age and become more overweight, they are at higher risk of

developing OA. Injuries to the knee joint, including the articular cartilage and other structures, can also lead to OA. However, due to the lack of vascularization in cartilage, healing of lesions can be prolonged or impossible. As a result, researchers have placed a significant emphasis on tissue engineering techniques to accelerate the recovery process using minimally invasive procedures [1,6].

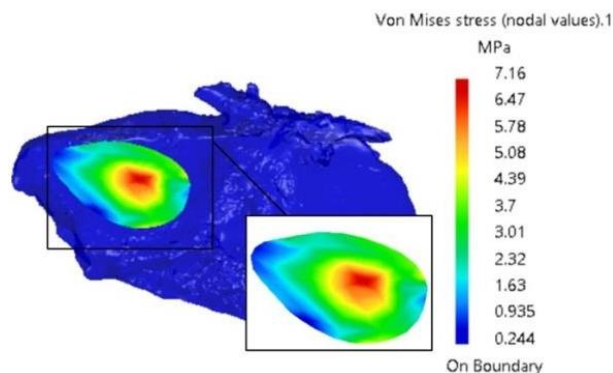


Fig. 8. Von Misses stress on reconstructed tibial cartilage.

Tissue engineering is not the only approach being investigated for improving cartilage repair; there is also growing interest in 3D printing technology. This is due to its success in enabling control over the geometry and internal structure of the scaffold tissue. To achieve successful integration of these technologies, it is important to achieve a balance of factors such as biological activity, mechanical strength, ease of production, and control of material degradation. This can be achieved through the combination of natural and synthetic materials [21].

Obtaining the exact shape of the damage is essential for creating the ideal structure to replace the filling of the lesion. To explore the possibilities of achieving the precise form of damage, many authors have segmented bones of animal origin (on which they induced corresponding injuries), bone sections during surgical interventions, cadavers, or bones reconstructed using MRI or CT images for research purposes [9,12,13,22]. In our study, we used a section of the tibial plateau with damage caused by degenerative disease (i.e. OA) after total knee arthroplasty.

A virtual reconstruction of the tibial plateau was created using a point cloud obtained by 3D scanning. Similar to our approach, B. Gatenholm et al. also reconstructed the tibial

plateau and the damage to the cartilaginous tissue [9]. The effectiveness of 3D scanning was also demonstrated in the research conducted by N.H. Trinh et al. [13].

As mentioned previously, it is crucial to accurately reconstruct the form of tissue damage. For example, Li et al. determined the volume of the defect by first scanning healthy bone, then creating damage and rescanning the bone. The volume of the defect was determined by subtracting the point clouds of the healthy and damaged bone [12]. In contrast, Gatenholm et al. filled the point cloud of the scanned object to define the original form of the damage [9]. In our study, we defined the wear volume by creating a Non-Uniform Rational B-Spline (NURBS) surface within the contour that represents the boundary between the damaged and healthy cartilage. Since both the curve and NURBS surface are parametrically described, it is possible to optimize either the curve or surface to achieve the best possible reconstruction results of the native knee through simulation analysis.

Comparing the worn surface area of the lateral lesion to the results obtained by Y. Wang et al., it can be concluded that approximately 50% of the tissue is damaged due to OA [23]. The total area of the damaged lesion is 2023.6 mm², while the total wear volume is 1.74 ml. These findings are consistent with the results obtained by N.H. Trinh et al. [13], further supporting the notion that about 50% of the tissue is damaged due to OA in this case.

Due to the complex nature of OA, it is essential to analyze stresses in both real and approximate conditions to evaluate the behavior of reconstructed lesions, perform comparative analyses, and make necessary corrections. Similarly to K.A.H. Myller et al., we performed a standing-phase FEM analysis of damaged and reconstructed cartilage on the tibial plateau [22]. The results show that, in real circumstances, maximum stresses are oriented anteriorly and medially due to the deformities present within the knee joint. After reconstructing the lesion, a clear reduction and even distribution of stress can be observed from the center to the outer sides of the lateral condyle of the tibial plateau [14, 22].

5. CONCLUSION

In this paper, we have presented a methodology for reconstructing worn cartilage on the tibial plateau caused by the presence of OA. Additionally, we have conducted an FEM analysis on the tibial plateau, both on the damaged and reconstructed lateral condyle. By utilizing this methodology for reconstructing tissue damage, it is possible to create custom-made implants quickly, easily, and efficiently with as few invasive procedures as possible. Assessing tribological and mechanical parameters within the knee joint can greatly assist physicians in clinical diagnostic procedures, treatment, and rehabilitation decision-making. Our future research aims to create a digital anatomical atlas that will contain estimated volumes, surfaces, and masses of wear based on the category and location of OA.

REFERENCES

- [1] M. Mostakhdemin, A. Nand, M. Ramezani, *Articular and Artificial Cartilage, Characteristics, Properties and Testing Approaches - A Review*, Polymers, vol. 13, no. 12, pp. 1-25, 2021, doi: [10.3390/polym13122000](https://doi.org/10.3390/polym13122000)
- [2] M.E. Mononen, M.K. Liukkonen, R.K. Korhonen, *Utilizing Atlas-Based Modeling to Predict Knee Joint Cartilage Degeneration: Data from the Osteoarthritis Initiative*, Annals of Biomedical Engineering, vol. 47, pp. 813-825, 2019, doi: [10.1007/s10439-018-02184-y](https://doi.org/10.1007/s10439-018-02184-y)
- [3] P. Čípek, D. Rebenda, D. Nečas, M. Vrbka, I. Křupka, M. Hartl, *Visualisation of Lubrication Film in Model of Synovial Joint*, Tribology in Industry, vol. 41, no. 3, pp. 387-393, 2019, doi: [10.24874/ti.2019.41.03.08](https://doi.org/10.24874/ti.2019.41.03.08)
- [4] A. Siddiqi, H. Anis, I. Borukhov, N.S. PiuZZi, *Osseous Morphological Differences in Knee Osteoarthritis*, Journal of Bone and Joint Surgery, vol. 104, no. 9, pp. 805-812, 2022, doi: [10.2106/JBJS.21.00892](https://doi.org/10.2106/JBJS.21.00892)
- [5] L.P. Bartsch, M. Schwarze, J. Block, M. Alimusaj, M. Schiltenwolf, A. Jaber, S.I. Wolf, *Varus Knee Limits Pain Relief Effects of Laterally Wedged Insoles and Ankle-Foot Orthoses in Medial Knee Osteoarthritis*, Journal of Rehabilitation Medicine, vol. 54, pp. 1-9, 2022, doi: [10.2340/jrm.v54.1129](https://doi.org/10.2340/jrm.v54.1129)
- [6] K.D. Allen, L.M. Thoma, Z.M. Golightly, *Epidemiology of osteoarthritis*, Osteoarthritis and Cartilage, vol. 30, pp. 184-195, 2022, doi: [10.1016/j.joca.2021.04.020](https://doi.org/10.1016/j.joca.2021.04.020)

- [7] P.A. Sukerkar, Z. Doyle, *Imaging of Osteoarthritis of the Knee*, Radiologic Clinics of North America, vol. 60, iss. 4, pp. 605-616, 2022, doi: [10.1016/j.rcl.2022.03.004](https://doi.org/10.1016/j.rcl.2022.03.004)
- [8] N. Prodanovic, S. Petrović Savic, G. Devedzic, A. Matic, D. Radovanovic, B. Ristic, *Comparative gait analysis of patients with different design of total knee arthroplasty*, Serbian Archives of Medicine, vol. 149, no. 9-10, pp. 579-584, 2021, doi: [10.2298/SARH200706046P](https://doi.org/10.2298/SARH200706046P)
- [9] B. Gatenholm, C. Lindahl, M. Brittberg, S. Simonsson, *Collagen 2A Type B Induction after 3D Bioprinting Chondrocytes In Situ into Osteoarthritic Chonral Tibial Lesion*, Cartilage, vol. 13, iss. 2, pp. 17555-17695, 2020, doi: [10.1177/1947603520903788](https://doi.org/10.1177/1947603520903788)
- [10] V.L. Popov, A.M. Poliakov, V.I. Pakhaliuk, *Synovial Joints, Tribology, Regeneration, Regenerative Rehabilitation and Arthroplasty*, Lubricants, vol. 9, iss. 2, pp. 15, 2021, doi: [10.3390/lubricants9020015](https://doi.org/10.3390/lubricants9020015)
- [11] B. Swain, S. Bhuyan, R. Behera, S. S. Mohapatra, A. Behera, *Wear: A Serious Problem in Industry* in A. Patnaik (Ed.): Tribology in Materials and Manufacturing - Wear, Friction and Lubrication, IntechOpen, 2021, doi: [10.5772/intechopen.94211](https://doi.org/10.5772/intechopen.94211)
- [12] L. Li, F. Yu, J. Shi, S. Shen, H. Teng, J. Yang, X. Wang, Q. Jiang, *In Situ Repair of Bone and Cartilage defects Using 3D scanning and 3D printing*, Scientific Reports, vol. 7, 2017, doi: [10.1038/s41598-017-10060-3](https://doi.org/10.1038/s41598-017-10060-3)
- [13] N.H. Trinh, J. Lester, B.C. Fleming, G. Tung, B.B. Kimia, *Accurate measurement of Cartilage Morphology Using a 3D Laser Scanner*, in: R.R. Beichel, M. Sonka (Eds): Computer Vision Approaches to Medical Image Analysis, Springer, pp. 37-48, 2006, doi: [10.1007/11889762_4](https://doi.org/10.1007/11889762_4)
- [14] A. Mohammadi, K.A.H. Myller, P. tanska, J. Hirvasniemi, S. Saarakkala, J. Toyras, R.K. Korhonen, M. E. Mononen, *Rapid CT-based Estimation of Articular Cartilage biomechanics in the Knee Joint Without Cartilage Segmentation*, Annals of Biomedical Engineering, vol. 48, iss. 12, pp. 2965-2975, 2020, doi: [10.1007/s10439-020-02666-y](https://doi.org/10.1007/s10439-020-02666-y)
- [15] M.D. Kohn, A.A. Sassoon, N.D. Fernando, *Classification in brief: Kellgren-Lawrence classification of osteoarthritis*, Clinical Orthopedics and Related Research, vol. 474, no. 8, pp. 1886-1893, 2016, doi: [10.1007/s11999-016-4732-4](https://doi.org/10.1007/s11999-016-4732-4)
- [16] F. Moreira-Izurieta, A. Jabbarzadeh, *Tribological Studies in Cartilaginous Tissue of Lamb Sznovial Joints Lubricated by Distilled Water and Interstitial-Fluid-Like Solution*, Tribology in Industry, vol. 39, no. 3, pp. 319-328, 2017, doi: [10.24874/ti.2017.39.03.06](https://doi.org/10.24874/ti.2017.39.03.06)
- [17] K. Panchuk, T. Myasoedova, E. Lybchinov, *Spline Curves Formation Given Extreme Derivates*, Mathematics, vol. 9, iss. 1, pp. 1-29, 2021, doi: [10.3390/math9010047](https://doi.org/10.3390/math9010047)
- [18] R.M. Obradovic, *Descriptive-Geometrical Methods in Computer Graphics: The Intersection between Two Surfaces of Revolution by Use of Common Spheres and Common Planes*, PhD thesis, Faculty of Sciences University of Novi Sad, Novi Sad, 2000.
- [19] P.Đ. Milić, *Development of isogeometric finite element method and its application in structural analysis of transport machines*, PhD thesis, Faculty of Mechanical Engineering University of Niš, Niš, 2018.
- [20] A.S. Chandran, R. Trivedi, B. Modi, R. Patel, *Estimation of Stress and Strain of Knee joint Using Finite Element Analysis*, Journal of Physics: Conference Series, vol. 2070, iss. 1, id. 012217, 8 pp, 2021, doi: [10.1088/1742-6596/2070/1/012217](https://doi.org/10.1088/1742-6596/2070/1/012217)
- [21] L. Zhang, G. Yang, B.N. Johnson, X. Jia, *Three-dimensional (3D) printed scaffold and material selection for bone repair*, Acta Biomaterialia, vol. 84, pp. 16-33, 2019, doi: [10.1016/j.actbio.2018.11.039](https://doi.org/10.1016/j.actbio.2018.11.039)
- [22] K.A.H. Myller, R.K.K. Korhonen, J. Töyräs, P. Tanska, S.P. Väänänen, J.S. Jurvelin, S. Saarakkala, M.E. Mononen, *Clinical Contrast-Enhanced Computer Tomography with Semi-Automatic Segmentation provides Feasible Input for Computational Models of the Knee Joint*, Journal of Biomechanical Engineering, vol. 142, iss. 5, 2020, doi: [10.1115/1.4045279](https://doi.org/10.1115/1.4045279)
- [23] Y. Wang, A.E. Wluka, F.M. Cicuttini, *The Determinants of Change in Tibial Plateau Bone Area in Osteoarthritic Knees: A Cohort Study*, Arthritis Research & Therapy, vol. 7, iss. 3, pp. 687-693, 2005, doi: [10.1186/ar1726](https://doi.org/10.1186/ar1726)